Available online at www.sciencedirect.com

ScienceDirect

IFAC Papers Online
CONFERENCE PAPER ARCHIVE

IFAC-PapersOnLine 48-21 (2015) 1451–1456

Off-the-Grid Compressive Sensing for Broken-Rotor-Bar Fault Detection in Squirrel-Cage Induction Motors

Dehong Liu * **Dingguo Lu** **,[1]

* *Mitsubishi Electric Research Laboratories, Cambridge, MA 02139 USA (e-mail: liudh@merl.com)*
** *University of Nebraska-Lincoln, Lincoln, NE 68588, USA (email: stan1860@huskers.unl.edu)*

Abstract: In this paper, we propose an off-the-grid compressive sensing based method to detect broken-bar fault in squirrel-cage induction motors. To validate our method, we first build a dynamic model of squirrel-cage induction motor using multi-loop equivalent circuit to simulate motor current under fault conditions. We then develop an off-the-grid compressive sensing algorithm to extract the fault characteristic frequency from the simulated motor current by solving an atomic norm minimization problem. Comparing to other fault detection methods via motor current signature analysis, our method yields high resolution in extracting low-magnitude fault characteristic frequency with only 0.7 second measurements. Simulation results validate our proposed method.

Keywords: Fault detection, broken bar, squirrel-case induction motor, compressive sensing

1. INTRODUCTION

The squirrel-cage induction motors suffer from a variety of mechanical and electrical faults, of which about 10% are related to broken-rotor-bar(BRB) fault Zhang et al. (2011). The BRB fault can be caused by either imperfections in the manufacturing process, or non-smooth operations such as direct-on-line starting duty cycles and pulsating mechanical loads. Although the BRB fault generally does not lead to instant failures to the induction motors, it causes serious secondary effects, such as excessive vibrations, poor starting performance, and torque fluctuation, *etc*. Even worse, the broken part may hit stator windings at high velocity, causing catastrophic failures on winding insulation. Therefore, it is of great importance to detect the BRB fault in time so as to reduce the cost of maintenance and repair Santos et al. (2006).

In order to detect the BRB fault, signatures are extracted from motor current, air-gap flux, torque, and vibration, *etc*, for further analysis. Among these fault signatures, motor current signature is gaining more attention for its non-invasiveness and low cost. When there exists a BRB fault in the squirrel-cage induction motor, the rotor operates asymmetrically, inducing extra frequency components $f_{sb} = (1 \pm 2\kappa s) f_s$ in the stator current Filippetti et al. (1998), where s is the speed slip, typically ranges from 0.005 to 0.05 under steady operating condition; f_s is the power supply frequency; and $\kappa = 1, 2, 3, ...$ is the harmonic frequency index. Among these extra components, the $(1 - 2s) f_s$ component is the strongest one and typically treated as the indicator of a BRB fault. Thus frequency $(1 - 2s) f_s$ is also termed the characteristic frequency. BRB fault detection via motor current signature analysis(MCSA) is basically detecting the characteristic frequency component $(1 - 2s) f_s$.

However, it is challenging to detect the characteristic component due to the following factors. First, the magnitude of characteristic frequency is relatively small, typical 30∼40dB lower than that of the fundamental power supply frequency. Second, the characteristic frequency $(1 - 2s) f_s$ is very close the power supply frequency f_s. Under steady operating condition, the frequency distance between the characteristic frequency and the fundamental frequency f_s can be as small as $0.01 f_s$. It is generally difficult to distinguish the characteristic frequency from the fundamental frequency using the traditional Fourier spectral analysis. Although a big extension of measurement time may be helpful, it requires near constant load to ensure both the slip and motor current remain stable during the whole measurement period, otherwise the load fluctuation will interfere the accuracy of fault detection. This constant load requirement in many cases can be troublesome because the unavoidable load fluctuation in reality especially over a long measurement period. Therefore, it is necessary to develop a high frequency resolution analysis method using very short time measurements to meet the real situations in BRB detection.

In the past decades, researchers have developed different MCSA methods such as Fourier transform spectral analysis, short-time Fourier transform Bellini et al. (2001); Zhao and Lipo (1996); Toliyat and Lipo (1995) and subsequent high resolution spectral analysis using ESPRIT Xu et al. (2012) and MUSIC Kim et al. (2013). Although existing methods can achieve high resolution in BRB detection,

[1] Initial work was done while Dingguo Lu was an intern with Mitsubishi Electric Research Laboratories, 201 Broadway, Cambridge, MA 02139, USA.

2405-8963 © 2015, IFAC (International Federation of Automatic Control) Hosting by Elsevier Ltd. All rights reserved.
Peer review under responsibility of International Federation of Automatic Control.
10.1016/j.ifacol.2015.09.729

they have several limits. First, they still require seconds of measurements under constant load. Any load fluctuation within the measurement period could interfere the accuracy of fault detection. Second, they are not capable of detecting early-stage fault, of which the characteristic frequency component is very weak.

In recent years, the development of compressive sensing (CS) provides us a feasible solution to analyze high resolution frequency components even with few measurements. Compressive sensing is an innovative method to capture and represent sparse or compressible signals at a rate well below its Nyquist sampling rate Baraniuk (2007); Candès and Wakin (2008). This sampling rate reduction is achieved by measuring uncorrelated or randomized projections of the sparse signals and reconstructing the sparse signal using improved signal models and nonlinear reconstruction algorithms. In spectral analysis this sampling rate reduction means with a fewer amount of measurements, we are able to reconstruct the same resolution frequency spectrum, or with the same amount of measurements but higher resolution than the traditional methods. In MCSA based fault detection, the motor current spectrum with fault characteristic frequency exhibits sparse characteristics in the frequency domain. Therefore, the characteristic frequency component can be resolved with high resolution using compressive sensing based techniques. Considering the fact that the characteristic frequency is distributed in the *continuous* frequency domain, we consider the off-the-grid compressive sensing technique Tang et al. (2013).

In order to verify our method, we build a dynamic model using multi-loop equivalent circuit to simulate stator current, in which a broken bar fault is modeled by an open circuit while an early stage broken-bar fault is simulated using an increased resistance of the fault branch. We then develop an off-the-grid compressive sensing algorithm to extract the characteristic frequency component in the simulated stator current.

This paper is organized as follows. In Section 2, we describe the dynamic model of induction machine for stator current simulation under healthy and fault conditions. In Section 3, we introduce compressive sensing fundamentals and our off-the-grid compressive sensing algorithm. Fault detection results on simulated data are presented in Section 4. Finally, we draw conclusions in Section 5.

2. DYNAMIC MODEL OF INDUCTION MOTOR

In squirrel-cage induction motors, the stator consists of three sinusoidally distributed windings, displaced by 120° spatial angle. The rotor contains longitudinal conductive bars connected at both ends by shorting rings, forming a squirrel-cage like shape. As the induction motor is operating, the stator windings set up a rotating magnetic field through the rotor, inducing electrical current in the rotor bars, producing force acting at a tangent orthogonal to the rotor, and resulting in torque to turn the shaft.

In the following part of this section, we first develop a dynamic model for motors in normal healthy condition, then extend it to fault conditions. For simplicity, we neglect magnetic saturation and assume linear magnetic characteristics.

The equivalent circuit of squirrel-cage induction motor is shown in Fig.1. Assuming there are n rotor bars, the squirrel-cage rotor can then be modeled as $n+1$ independent current loops, where n of them are identical circuit loops under ideal condition, with each loop consisting of two adjacent rotor bars connected by two end ring portions. The remaining circuit loop is formed by one of the end rings. So, the current distribution in rotor can be specified in terms of $(n+1)$ independent loop currents, *i.e.*, n rotor-bar loop currents i_j $(1 \le j \le n)$ plus one end ring loop current i_e.

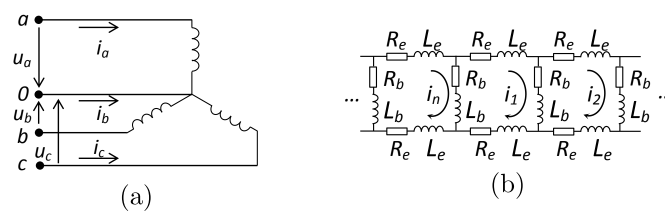

Fig. 1. Equivalent circuit of (a)stator windings, and (b)rotor in squirrel-cage induction motor

2.1 Stator Voltage and Flux Equations

Based on the equivalent circuit, the voltage and flux linkage equations for the stator windings can be written as:

$$\mathbf{U}_s = \mathbf{R}_s\mathbf{I}_s + \frac{d\mathbf{\Psi}_s}{dt}, \tag{1}$$

$$\mathbf{\Psi}_s = \mathbf{L}_s\mathbf{I}_s + \mathbf{M}_{sr}\mathbf{I}_r, \tag{2}$$

where the stator voltage

$$\mathbf{U}_s = [u_a \ u_b \ u_c]^T, \tag{3}$$

with

$$u_a = U_0 \cos(2\pi f_s t + \phi_0), \tag{4}$$

the stator current

$$\mathbf{I}_s = [i_a \ i_b \ i_c]^T, \tag{5}$$

the stator winding flux

$$\mathbf{\Psi}_s = [\psi_a \ \psi_b \ \psi_c]^T, \tag{6}$$

the stator resistance

$$\mathbf{R}_s = \begin{bmatrix} R_s & 0 & 0 \\ 0 & R_s & 0 \\ 0 & 0 & R_s \end{bmatrix}, \tag{7}$$

the stator inductance

$$\mathbf{L}_s = \begin{bmatrix} L_s & M_{ab} & M_{ac} \\ M_{ba} & L_s & M_{bc} \\ M_{ca} & M_{cb} & L_s \end{bmatrix}, \tag{8}$$

the stator-rotor mutual inductance

$$\mathbf{M}_{sr} = \begin{bmatrix} m_{a1} & m_{a2} & \cdots & m_{an} & m_{ae} \\ m_{b1} & m_{b2} & \cdots & m_{bn} & m_{be} \\ m_{c1} & m_{c2} & \cdots & m_{cn} & m_{ce} \end{bmatrix}, \tag{9}$$

and the rotor current

$$\mathbf{I}_r = [i_1 \ i_2 \ \cdots \ i_n \ i_e]^T. \tag{10}$$

Here we use bold capital letters for matrices, regular capital letters for constant parameters and small letters for time-variant parameters. It is important to note that the stator winding resistance in (7) and the inductance of